

Final Design Report

Team 5 - Lamarvelous

AAE 451 - Senior Design; Aircraft Design Build Fly

By Nathon Carey, Aidan Doyle, Mike Flanagan, Max Gorlich, Jose Lara,
Ashwin Nathan, and Dhruv Wadhwa.

Table of Contents

Executive Summary.....	3
High Level Requirements.....	3
Best Aircraft Concept.....	5
Comparison to Baseline Aircraft.....	5
Walkaround Chart.....	6
Downselection.....	6
Advanced Aircraft Description.....	8
Structures and Weights.....	9
Flight Performance.....	18
Parts Acquisition List.....	21
Prototype Fabrication, Economic, and Test Plan.....	21
As-Built Aircraft Description.....	23
Flight Test Data Tables.....	23
Vehicle Manufacturing.....	23
Design Modifications Post CDR.....	28
Description of Flight Test.....	29
Key Lessons Learned.....	29
Appendix.....	30

Executive Summary

In this project, our team designed, built, and flew a remote-controlled aircraft around a preconceived flight course. There are several project milestones that we utilized over the course of the semester to show the progression of our design and share any and all major engineering decisions we make, including the SRR + SDR (System Requirement and Design Reviews) milestone, as well as the CDR (Conceptual Design Review). This milestone is the final report, written after the successful flight of our aircraft and completion of the mission. This report will be discussing the high level requirements, our aircraft concept, the down-selection process between our promising concepts, and an advanced description of our design. In addition, we will also be discussing a number of quantitative specifications, including the sizing, weights, structures, aerodynamics, propulsion, and stability/controls. Finally, this report will also be detailing steps taken after CDR, including the fabrication and manufacturing process, key changes that were made during this process, justification explaining why those changes had to be made, a discussion over our the results of the flight test, and key takeaways the team was able to grasp from this project. After fabrication, the empty weight of our aircraft was 5.69 lbs. With our battery and payload (14 cubes at 2.18 oz each) the weight of our aircraft was 8.66 lbs. Our aircraft was able to complete the mission successfully, and achieved a flight time of 90 seconds, giving us a final score of 0.339 oz/sec. The final cost of the aircraft was \$385.42, keeping the team's cost within the given budget.

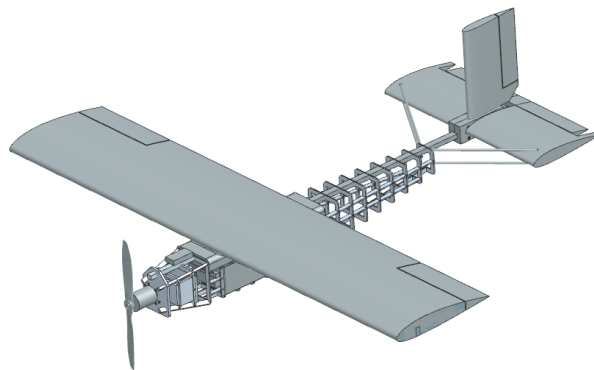


Figure 1: Final Aircraft CAD

High Level Requirements

A flight “score” is determined after flight tests based on the following equation:

$$\text{Score} = \text{Payload Weight} / \text{Time to Complete Course}$$

Many requirements are imposed on our design that come directly from the RFP, however, we also chose to develop our own requirements to guide us to build a well performing and high scoring aircraft for flight tests. The following list of requirements were those directly from the RFP:

- The aircraft shall be remotely piloted.
- The aircraft shall be propeller driven.
- The aircraft shall contain a fixed wing structure.
- The aircraft shall be capable of being launched by hand; there will be no rolling takeoff.
- The aircraft shall be capable of performing a belly landing.
- Aircraft shall at least have the range to complete three laps around a predetermined airfield course at McAllister Park.
- The aircraft shall be stored within a 30 in width x 30 in height x 60 in length storage volume.
- The aircraft wingspan shall be a maximum of 5 ft.
- After takeoff, the aircraft shall climb to a maximum altitude of 200 ft.
- The aircraft shall be easy to assemble, deploy and fly onsite; preflight construction time must be minimal.
- The payload and battery onboard the aircraft shall be easily and quickly swappable.
- The aircraft shall be stable under all flight conditions.
- The aircraft shall be easy to fly by a pilot external to the team.
- All teams shall use a standardized payload (weight and dimensions are equivalent per payload).
- All teams shall implement the same six-channel receiver and transmitter into their design.

- The maximum budget for materials and construction shall be 400\$.

These requirements from the RFP gave our group a good starting point to begin a concept generation process. However, after design iteration and brainstorming, we realized we needed to further create and expand our requirements list to be more thorough and specific for the overall purpose of this design process. The following are requirements we felt were necessary to add, along with our rationale for their additions:

System, Performance, or Operational	Requirement	Threshold Value	Target Value	Rationale for Target	Final Value Achieved
System	The weight of the aircraft shall not exceed 30 lbs with payload.	30 lbs	15 lbs	Previous aircrafts were well under this weight. This will allow ease of handling compared to a larger aircraft.	8.66
Operational	The aircraft shall withstand and function in temperatures as low as 20 degrees fahrenheit.	20 °F	15 °F	Flight testing will occur during November, and although the weather will be hard to predict exactly, it would be better to prepare for colder weather.	Test day temperature was in the 30s
Operational	The LiPo battery shall not be discharged below 3.2 V/cell. The team will decide on a minimum value to discharge at a later date.	3.2 V/cell		LiPo batteries and performance will degrade when the battery is discharged below this value, so we will keep a buffer to avoid this.	Never Discharged that low
System	The aircraft shall include at least one unit of payload (one unit = 0.13625 pounds, 1 inch steel cube with 5% manufacturing tolerances).	1 payload cube	15 payload cubes	The score of the mission is determined by the payload weight over the time of flight. To achieve a decent score, as well as have the aircraft weigh enough, we will theorize we will use this amount of payload.	14 Payload cubes
System	The aircraft shall be relatively easy to construct and assemble.	n/a	n/a	We do not have experience building RC planes, so our concept should be simple and easy to construct	Assembled under 5 mins
Performance	Aircraft C_{D_0} shall be determined with the goal in mind to minimize parasitic drag during flight.	0.02	0.03	This value of parasitic drag coefficients will be used to form both our power constraint and our maneuvering constraint.	0.0348
Performance	Aircraft L/D_{max} shall be chosen to maximize our efficiency with the climb rate of our aircraft.	16	14	This value of $(L/D)_{max}$ values will be used to form our climb constraint.	12.5
Performance	Aircraft stall $C_{L,max}$ shall be at a value that allows the plane to maximize efficiency at stall speed.	1.3	1.4	The baseline $C_{L,max}$ value will be used to form our stall constraint.	1.4

Table 1: Internally derived requirements and rationales for their inclusion.

CONOPS

Our concept of operations has not had any major changes since SRR and SDR. We still plan the same mission around the airfield while carrying a payload. We plan to hand launch the aircraft, climb up to cruise altitude under 200 ft, complete 3 laps, and belly land. The only potential update is to our turning phase, where we are considering slowing down under our cruise speed to allow for greater control of the aircraft and a faster turn.

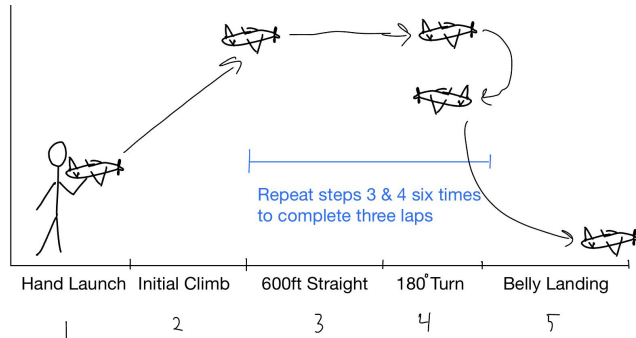


Figure 2: Concept of Operations

Best Aircraft Concept

After downselection, we decided that the best aircraft given our mission, requirements, CONOPS, and other criteria was a single engine, high wing puller aircraft. The following tables detail our design parameters and a comparison to a similar RC aircraft in the market now.

Design Parameters of Best Design	
Gross Weight	8.66 lb _f
Payload	1.91 lb _f
Wing Loading	1.445 lb _f / ft ²
Wing Area	5.64 ft ²
Wing Aspect Ratio	4.71
Thrust to Weight	1.15
Cost	\$385.42

Table 2: Design Parameters

Comparison to Baseline Aircraft

The major comparison between the baseline aircraft and ours were the payload capacity, ease of assembly and cost. Our plane was designed to maximize payload capacity as that was the goal of the mission but the baseline aircraft has almost no capacity for payload with just enough space for controls. The baseline aircraft is also much lighter and costs less as it is built by a manufacturer at scale while our design was built as a single product. Even then the cost difference is not too different. Our plane has storage mode with the main wing being easily separated that can also be assembled on site in under 5 minutes while the assembly time for the baseline aircraft is 15 ins. Our plane is less controllable as our design does not include flaps for the wings but the baseline aircraft does. Our design is more durable as it is made out of wood and 3d printed parts while the baseline aircraft is completely made out of foam. Our performance in terms of speed might be lower but our design would perform better at the mission due to our capability to carry a much higher amount of payload.

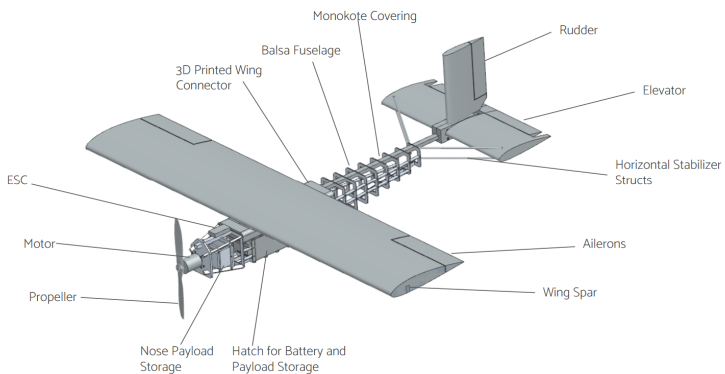
Criteria	Baseline Aircraft Skynetic Shrike Glider	Our Design
Cruise Speed	-	-

Payload	-	+
Ease of Assembly	-	+
Controllability	-	-
Cost	-	-
Durability	-	+
Scores + S -	-	3 0 3

Table 3: Comparison to Baseline

Walkaround Chart

This is our final design showing a single-engine puller with a high wing. Our plane follows rectangular wings for all airfoils due to ease of manufacturability. The fuselage is made out of balsa and the nose is made out of plywood to carry the weight of the nose and the battery. The wing and the tail sit on 3-D printed parts that connect them and the fuselage. The wing has a rectangular spar at the bottom quarter chord. The horizontal stabilizer has two internal circular spars. A hatch below the wing attaches with velcro and can be used to access the battery and payload. The ESC is kept on top of the nose for cooling reasons. Two horizontal stabilizer structs are on either side of the fuselage to keep the stabilizer stable. Lastly, the plane was covered using Monokote to provide a light solution to decrease the drag of the plane.

**Figure 3:** Walk Around Chart

Downselection

At the end of SRR+SDR after continuous iterations of brainstorming and doing the Pugh's Method, we were left with three aircraft concepts as seen below. The three designs were a High-Wing Twin Tractor, a Low-Wing Single Engine Puller, and a Blended Body Single Engine Pusher.

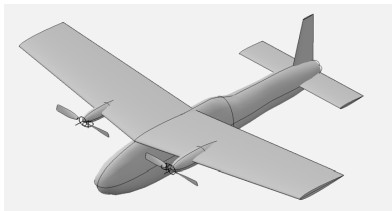
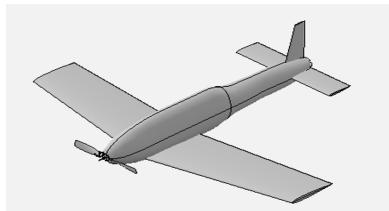
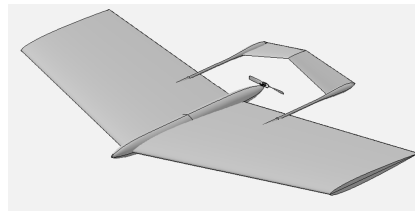
**High-Wing Double-Engine****Low-Wing Single-Engine****Blended-Body Single-Engine**

Figure 4: SRR+SDR Concepts

In SRR+SDR, we focused more on performance and mission goals. In CDR, as we approached manufacturing we had to consider the extremely short time to build the plane and the budget. Therefore, our primary focus was on cost, design complexity, and ease of construction, while carefully weighing trade-offs with performance. We performed qualitative analysis to choose the best design while focusing on these attributes.



Figure 5: Qualitative Analysis of Final Concepts

Combined View:

■ High-Wing Double-Engine ■ Low-Wing Single-Engine ■ Blended-Body Single-Engine

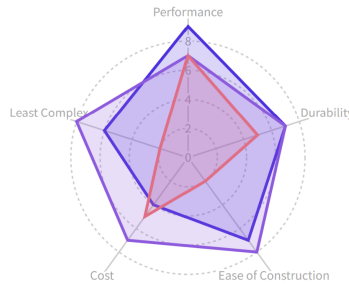


Figure 6: Qualitative Analysis of Final Concepts (Combined)

Looking at the diagram above it was clear to us that the blended body concept was simply not a concept we can pursue in this timeframe and budget and still have a high-performance aircraft. For that reason, the blended body was eliminated as an option for further consideration.

The other two designs that were left were the High Wing Twin Tractor and the Low Wing Single Engine Puller. The Low-Wing design did better on complexity, cost, and ease of construction than the High-Wing design but did not perform as well as the High-Wing as that design has two engines that would lead us to have much higher speed and perform the mission faster.

To establish a compromise between the concepts we decided to merge the two concepts. Taking the single engine puller from the Low-Wing, and making it a High-Wing we are able to balance performance with cost, complexity, and construction.

■ High-Wing Double-Engine ■ Low-Wing Single-Engine ■ High-Wing Single-Engine (Final Design)

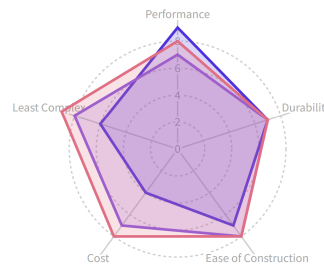


Figure 7: Qualitative Analysis including Final Design

Advanced Aircraft Description

The following are images of our CAD showing external layouts and internal layouts with dimensions including wing to nose, tail to wing, height, wing span, and wing chord.

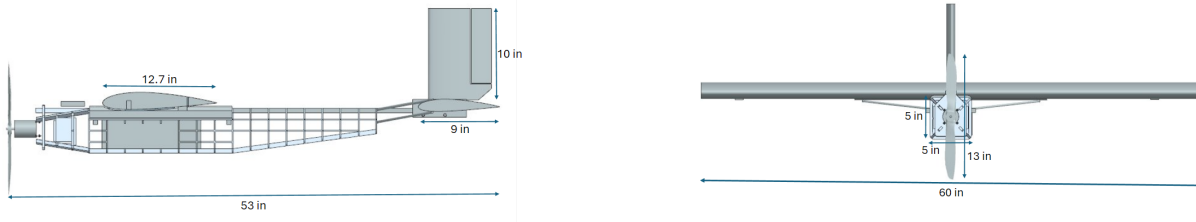


Figure 8: Various Views of Chosen Aircraft

The fuselage length is 53 in and the wing length is 60 in to satisfy the storage requirements of being under or equal to 60 in. The fuselage is separated into three separate parts: the nose, the storage, and the tail. The storage section is 5in by 5in cuboid made out of balsa and contains the battery and the payload. A hatch is present here for access. The nose section is tapered from the storage until it reaches a plate which holds the motor. The nose section is made out of plywood to better hold the motor and payload inside it. The tail section is also tapered and made out of balsa and only contains the wiring to the tail. These three parts are connected using spars that run along all these sections length wise and meet at the storage section where they are connected using a 3-D printed part and glue.

The wing is also connected on the same 3-D printed part using velcro and rubber bands. The wing chord is 12.7 in and has the same corresponding negative shape on the 3-D print allowing the wing to sit on the fuselage perfectly. The tail in the back is connected to the fuselage also using another 3-D print that allows both stabilizer's spars to run through it. The horizontal stabilizer chord is 9 in and the vertical stabilizer chord is 10 in. In the images below we get a more focused view of the wing and tail connections to the fuselage with the 3-D prints. The spar on the wing was about 0.5 in wide and 1 in high spanning completely across the wing with a length of 60 in.

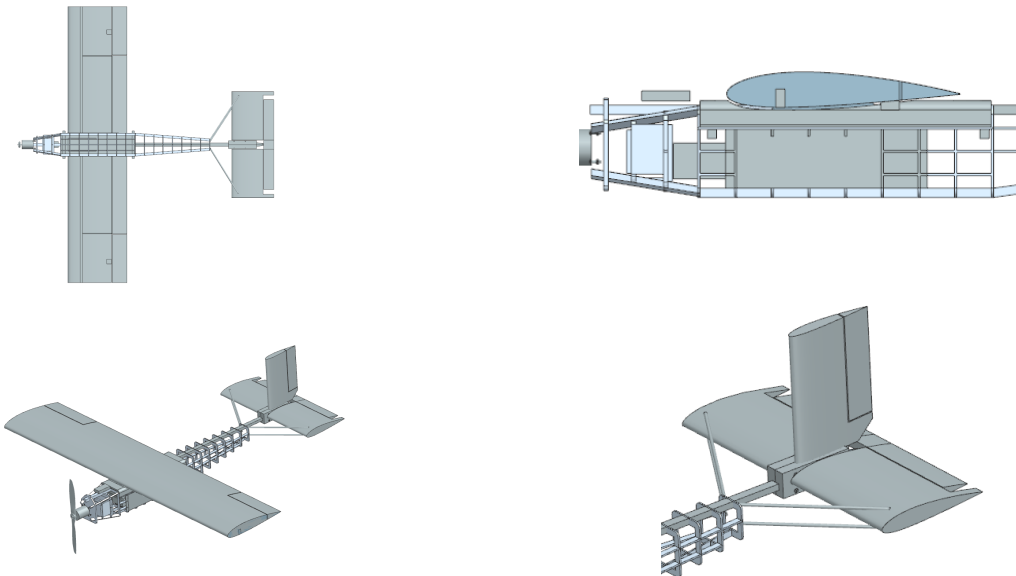


Figure 9: Other Angles of CAD

Sizing

As mentioned in previous reports, our sizing branches out from our constrain diagram, which using the equations listed below gave us our design space per the requirements of the project:

$$\frac{W}{S} = \frac{1}{2} \rho V_{Stall}^2 C_{L,max} = constant$$

$$\frac{W}{P_{SL}} = \frac{0.75 * 550}{\frac{1}{2} \rho_{SL} (1.1 C_{Do})} * \frac{\eta_p}{V_{cruise}^3} * \frac{W}{S}$$

$$\frac{W}{P} = \frac{550 \eta_p}{V_{climb} \left(\frac{1}{0.866 (\frac{L}{D})_{max} + \sin(\gamma)} \right)} = constant$$

$$\frac{W}{P} = \frac{550 \eta_p}{q V \left(\frac{C_{Do}}{W/S} + k \left(\frac{n}{q} \right)^2 \left(\frac{W}{S} \right) \right)}$$

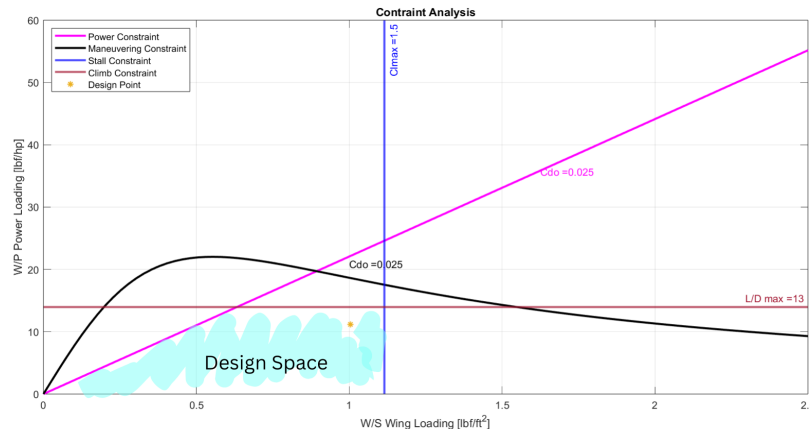


Figure 10: Constraint Diagram for High Wing Concept.

From this diagram using a 90% margin of error from the maximum allowable wing loading and power loading value, we determine our Wing loading to be 1.003 lb_f/ft² and our Power loading to be 11.141 lb_f/hp.

Structures and Weights

At the time of CDR, we chose to size our aircraft to carry 4 units of payload for the duration of the mission. This was a decision made early on with the help of the teaching team to ensure our estimated gross weight was below ten pounds. Our initial estimate with a 10% margin of error was 7.76 lb_f. Once we had constructed our aircraft, we realized that our center of gravity was too far back from our wing's quarter chord, and this required multiple design changes. This shift had occurred due to multiple structural changes close to our tail that had to be implemented due to the weak structural integrity of our laser cut balsa wood fuselage.

Through trial and error and multiple rounds of center of gravity testing, we determined that a new payload storage location with a total of 14 payload cubes both satisfied our desired thrust to weight ratio of bigger than one as well as our center of gravity location being close to our wings quarter chord. After a successful first flight test, we decided to maximize our payload carrying capacity with 29 total cubes. We had a secondary dedicated payload structure in a different location which allowed this test to have a very similar CG location as the first.

With this new design structure in mind and our new payload weight/amount, we were able to amend our previous report's group weight statement to more accurately reflect our final design. With this new weight layout and

new payload selection, our center of gravity was 4.18 inches aft of our wing's leading edge, and our chord length of 1.06 feet put our CG very close to our wing's quarter chord. As was the case in our last report, we decided that XFLR5 would be easier to represent our weight buildup, and would allow for a visual representation of our weights (approximated as point masses) and our center of gravity. Presented below is our group weight estimate as well as our XFLR5 mass buildup view:

	Weights (lbs)	Location(ft)	Moment(ft-lbs)
Structures	4.32		
Wing	1.76	1.68	2.96
Tail	0.86	4.5	3.87
Fuselage	1.70	1.5	1.49

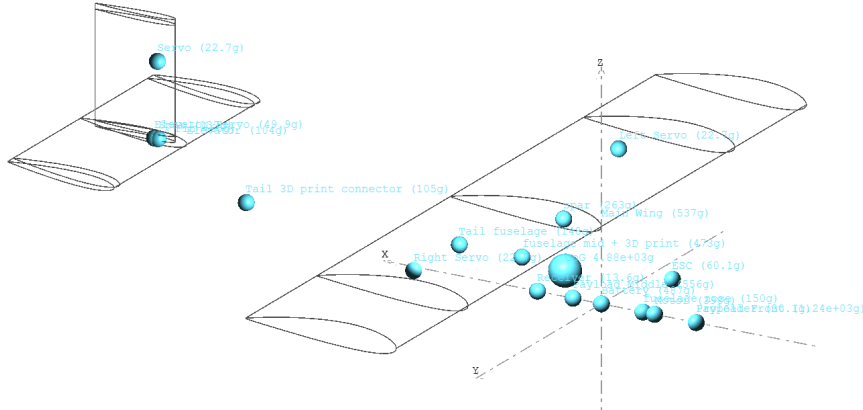
Propulsion	1.08		
Motor	0.88	0.18	0.16
ESC	0.13	0.84	0.11
Propeller	0.07	1.68	0.12

Equipment	0.29		
Aileron servos	0.10	2.28	0.23
Elevator	0.11	4.2	0.46
Rudder Servo	0.05	4.1	0.21
Receiver	0.03	2.13	0.06

Total Empty Weight	5.69		
--------------------	------	--	--

Useful Load	2.98		
Payload (14 units)	1.91	1.58	1.8
Battery	1.07	1.5	1.61

Total Gross Weight	8.66		
Finalized CG		4.18 inch	← Aft of LE

Table 4: Tabulated group weight statement (flight test accurate)**Figure 11:** Updated XFLR5 mass buildup view (flight test accurate).

Using XFLR5, we were also able to instantly obtain our moments and products of inertia:

I_{xx}	I_{yy}	I_{zz}	I_{xz}
3.27 lb _m ·ft ²	12.16 lb _m ·ft ²	10.95 lb _m ·ft ²	14.25 lb _m ·ft ²

Table 5: Updated Moments and product of inertia from XFLR5 (flight test accurate).

Figure V1 in our appendix shows our v-n diagram. The cruise velocity and dive velocity are shown to be about 40 ft/s and 55 ft/s respectively. These values differ from our intended cruise velocity of 77 ft/s. The v-n diagram numbers are derived from the equations given to us and our wing loading, so we believe they indicate that our intended cruise velocity will suffer from wing flutter. When we begin our flight tests we will be sure to look out for flutter, but these values do not raise concerns about our actual cruise velocity. The diagram also shows how wind gusts of 25 and 50 ft/s will affect our aircraft and stall lines. Figure V2 in our appendix shows how the limits mentioned in class apply.

Wing Load Analysis:

Our team simplified our wing to the basswood strut, which serves as a cantilever beam. This additional simplification is highly conservative, as it assumes that the foam portion of the wing gives and the rear spar provides no structural support. The team used the equations below to calculate moment and displacement. We assume uniform area and moment of inertia for the entirety of the wingspan.

$$V = \int q dx \quad M = \int V dx \quad \Theta = \int M/EI dx \quad D = \int \Theta dx$$

Assuming a cantilever beam, the wing tip has no shear and moment. Additionally, there is no deflection or angle at the root. The maximum bending and torsional loading conditions occur at the root. Maximum loading occurs during climb, and is approximated by the polyfit function below.

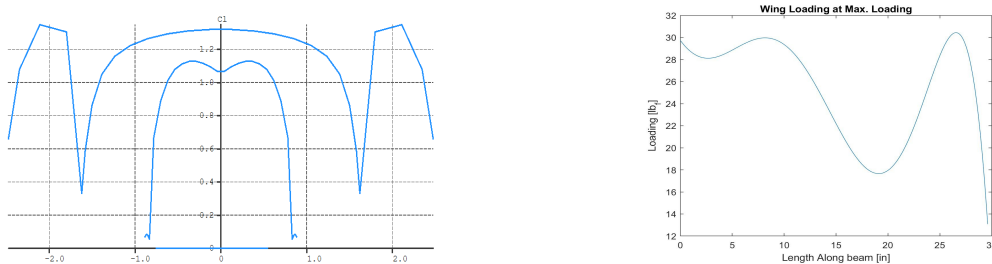


Figure 12: Wing loading from XFLR5 (left) and a MATLAB curve fit (right).

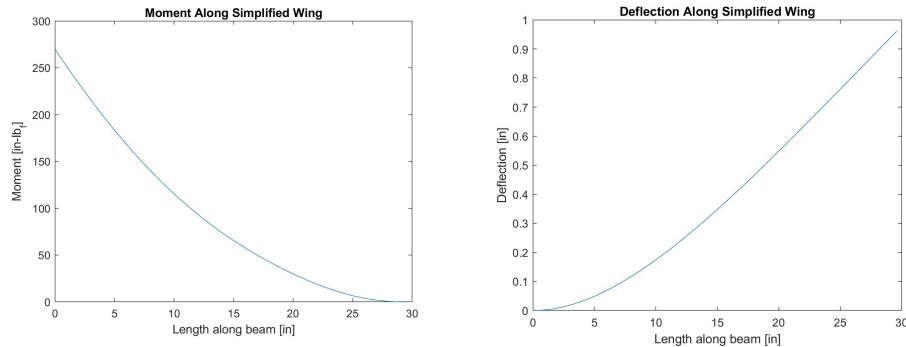


Figure 13: Moment and deflection along wing span.

At the wing root, there is a 270 in-lb moment. Assuming the moment occurs in the middle of the 1.25" spar, the max. compressive/tensile stress occurs 0.625" on the top/bottom of the spar. Using the moment equation $\sigma = -My/I$, the maximum stress is 3237 psi, which falls well within range for the 4730 psi compressive strength and 8700 psi bending strength.

The wing box comprises a 1"x1/2" basswood main spar at the 1/4 chord and a 0.5"x1/8" balsa spar at the 3/4 chord. The rear spar extends to the point where the ailerons begin. To ensure that the wing does not rotate by greater than 1 degree, the two spars are connected before the aileron by a piece of balsa. This will ensure limited rotation before the ailerons, which rotate depending on the control input. The basswood can conservatively handle 1.46 times the maximum wing loading shown above. This was calculated by dividing the compressive strength by the maximum root stress. The basswood can deflect about 1.4 inches before reaching compressive strength if this maximum loading occurs.

Material Selection:

For the fuselage, we are planning on using 1/8 inch thick balsa wood. Balsa wood is a light but relatively strong material, and is structurally sound enough to withstand aerodynamic forces. It is also relatively low in cost while also being easy to manufacture for our purposes. We will utilize ribs within the fuselage to keep the structure sound while also keeping weight low. We will also utilize one 1/2 inch by 1.25 inch rectangular wooden spar within the wing to increase stability of the wing itself. This will help counteract the critical loads placed on the wings and keep them safe. The tail will also utilize the spar that the wing does, and the vertical tail will not utilize extra structures to support loads.

For our wing, we will be using a NACA 2415 airfoil made of foam. This is low in cost and easy to manufacture. Based on past experiments using the foam, we will be reinforcing this material to make it stronger, which will be discussed later.

With regards to our tail, the horizontal stabilizer will be similar to the wing, but will be a NACA 0012 airfoil. For our vertical stabilizer, we will be using balsa wood again. We opted for balsa versus foam due to the fact that there will be a singular control surface, while the wing and horizontal stabilizer utilize two control surfaces. This means it needs to be more rigid for more controllability, and balsa wood is a better option because of this.

The wing-fuselage intersection for our high wing aircraft will utilize velcro and 8 rubber bands. A number of velcro strips will be placed on a 1/16 inch sheet of balsa wood above a divot at the top of the fuselage at the point of intersection. This divot will be deep enough to allow the leading edge and trailing edge of the airfoil to be flush with the top of the fuselage. These velcro strips will also be placed on the bottom of the airfoil at the point of intersection. These strips will be strong enough to keep the aircraft together during flight, but also allows for easy disassembly of the aircraft. In addition, we will utilize small pins on the sides of the fuselage to attach rubber bands in an x-shape, which will assist in keeping the airfoil attached to the fuselage.

The payload and battery will be placed between the nose and the leading edge of the airfoil. They will be placed within the fuselage, in a box large enough to carry both. This box will be closed by a small plank of balsa wood that will be held flush to the outer wall of the fuselage using velcro. This will allow for easy access as well as avoiding additional weight and cost.

Propulsion System

Process for Selection:

The main performance parameter that guided the selection process for our propulsion system was aiming for a thrust to weight ratio of around 1:1 after accounting for a 50% increase in total aircraft weight throughout the manufacturing process, which we will call out safety weight. This meant that, for an estimated aircraft weight of 7.672 lbf, our safety weight would be 11.508 lbf. The corresponding ideal thrust for a 1:1 thrust-to-weight ratio becomes 11.508 lbf.

Another major constraint that guided the process was hardware limitations in terms of battery selection. Most of the readily available and affordable hardware for RC aircraft (ESCs and motors) are compatible with LiPo batteries up to 6S cell configuration, thus setting an upper limit on the voltage the battery could provide.

Finally, using our constraint diagram, we needed to find a propulsion system capable of delivering enough mechanical power to satisfy our mission requirements. With a design power loading of 11.141 lbf/hp and using our safety weight, the calculated minimum mechanical power delivered to the propeller is equal to 1.032 hp.

Based on these 3 guiding selection principles, the final propulsion system components were chosen using eCalc, where we iterated through many components from common brands in order to satisfy these requirements, while trying to minimize both weight and cost. All calculations were made assuming an outside temperature of 40 F, what we expect to see during flight testing.

Selected System

Based on the requirements and constraints listed earlier, a battery was chosen that could deliver enough electrical power to the motor throughout the full length of the mission, plus a safety margin. The optimal battery turned out to be a Liperior 6S 3300 mAh, with a discharge rate of 30C and weight of 1.07 lbf. This battery is almost 3 times as heavy when compared to our initial estimate of 0.35 lbf based on historical data. Nonetheless, this tradeoff in weight means we are getting a lot more power and energy. Energy in Watt-hours is calculated as $Wh = Voltage \times Capacity$, where $Voltage = n \times 3.7$, where “n” is the number of cells in series, and capacity is in Ampere-hours (Ah). This results in a total energy stored of 73.26 Wh.

The propeller chosen is a 13in-diameter, 6.5in-pitch, 2-blade, APC Electric E propeller. The propeller is made out of injection-molded, long glass fiber composite with a nylon resin. The figures below show the performance parameters of the propeller as a function of advance ratio, at different rotational speeds. It is evident that, for all rotational speeds, the peak propeller efficiency occurs at an advance ratio of around 0.475. Moreover, the peak propeller efficiency is about 60%, which agrees with our initial guess that helped drive our constraint diagram.

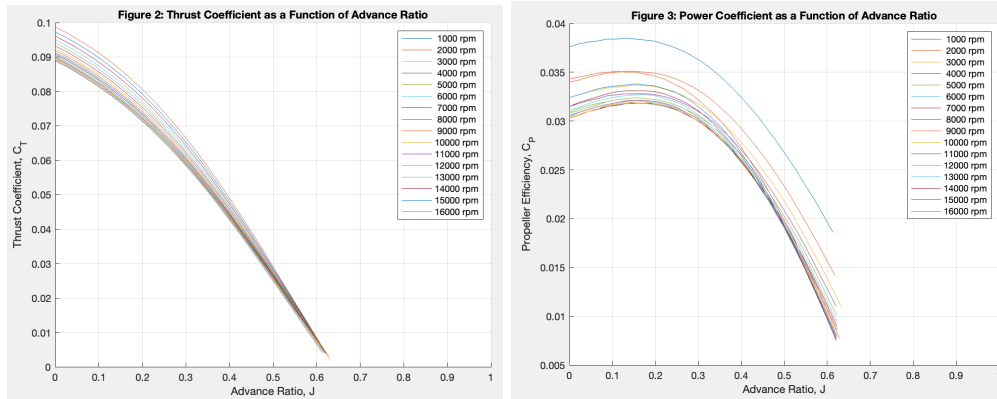


Figure 14: Thrust Coefficient vs Advance Ratio (Left) and Power Coefficient vs Advance Ratio (right)

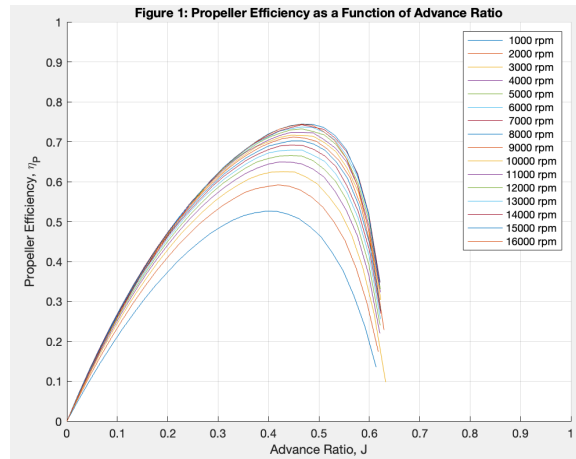


Figure 15: Propeller Efficiency vs Advance Ratio

The motor chosen to power our chosen propeller was a Cobra 4130/12 brushless motor. The motor's basic dimensions are an outer diameter of 1.961 in, and length of 2.433 in, with a total weight of 0.877 lbf. This motor can receive up to 1440 W of electrical power with a 6S battery, and is rated to a maximum continuous current of 65 A. The average motor efficiency is 91.6%, and the motor Kv is 540 RPM per volt.

Based on our mission requirements, thrust and power constraints, it was estimated that our best propulsion configuration drew 51.38 A of current at maximum performance. This meant that we needed an ESC capable of delivering at least 20% more than the max current draw, and supported a 6S LiPo battery. The chosen component was a RC Electric Parts 80A ESC.

The ESC chosen also outputs a BEC step down voltage of 5.5 at 4 amps. Our receiver and servos have a peak draw of 2.4 amps at this voltage, so our control systems will have ample power.

The component choices are summarized in the table below:

Battery	ESC	Motor	Propeller
Liperior 6S 3300 mAh 30C	RC Electric Parts 80A	Cobra 4130/12	APC 13x6.5E

Table 6: Propulsion system components.

Finally, all the major performance parameters are the following:

Parameter	Value
Energy [Wh]	73.26
Max Electric Power [hp]	1.400
Max Mechanical Power [hp]	1.282
Max Current Draw [A]	51.38
Static Thrust [lbf]	9.914
Thrust-to-weight Ratio	1.15
Max Flight Time [min]	4.8

Table 7: Propulsion system performance parameters.

Aerodynamics and Static Stability

Our aerodynamic analysis began with a component drag buildup using the methods presented in class. Our code that performs these calculations takes inputs from our defined concept geometry, the flight conditions, and the conceptual estimated weights for our aircraft. A test case was run to ensure proper performance of the code using the SR22 example from the lecture: the computed C_D from the lecture was 0.028, and the value found using our code was 0.02765 (this is a relative error of 1.25%). The code takes major components on an aircraft and estimates the experienced parasitic drag at some Reynolds number; it then adds this parasitic sum to an induced drag coefficient. The major components our code takes into account are the main wing, the horizontal and vertical tails, the fuselage, and any “miscellaneous” components, which the code estimates as 8% of the total parasitic drag coefficient. These components at cruise conditions gave us an estimated value for the parasitic drag and induced drag on our aircraft:

$$C_{D,0} = 0.0204, C_{D,i} = 0.00892$$

The code assumes no compressibility drag, which means our total estimated coefficient of drag is $C_D = 0.02934$. This value was used later in XFLR5 to get a more complete overview of our aerodynamic performance. With drag estimated, we moved on to size our wing, tails, and fuselage, and control surfaces.

When we built our aircraft, we were able to manufacture our wing using the hotwire foam cutter before it was broken, but we were unable to make our horizontal and vertical tail with the functioning cutter. We knew the precision required to manufacture our tail was far too high to be attempted by hand, so we decided to simplify our design. Rather than have a taper for both our tails, we decided to make rectangular tails using the mean chord length for both.



Figure 16: Modified XFLR5 views of Wing (Left) and Tail (right).

Our wing, tail, and fuselage sizing was all based on equations found in Raymer. The base of our geometric sizing comes from the following equation:

$$\text{Fuselage Length} = 3.5 * W_0^{0.23}$$

This equation is based on a singular variable, that being our aircraft's gross weight. At this stage in our design, we used our weight estimate from SRR+SDR using 4 units of payload: $W_0 = 7.76 \text{ lb}_f$. We used an equation from Raymer for placement of our wing relative to the nose of our aircraft: 40% length of fuselage from the nose to the quarter chord of the wing. We used an equation to find the length from the quarter chord of our wing to the quarter chord of our tail 60% length of fuselage from the quarter chord of our wing to the quarter chord of our tail.

We ran multiple XFLR5 studies to determine optimal wing configurations, and after concerns of manufacturability were sourced to our aero team, we decided that an unswept, untapered wing with no dihedral would fit the overall requirements of the project while still achieving the desired performance. We also iterated through designs using different airfoils for our wings and tails, and we decided that the NACA 2415 for our wing and the NACA 0012 for our tails were adequate. Geometric sizing of our wing was rather simple; our constraint diagram from SRR+SDR gave us an estimate for our wing loading ($W/S = 1.445$), and using this along with our gross weight estimate we were able to solve for the geometry of our wing.

$$S_w = W_0 / (W/S)$$

$$\text{Wing chord} = S_w / 5$$

We used estimates of tail volume coefficients to size our horizontal and vertical tail:

$$V_{Ht} = S_{Ht} * L_{Ht} / (S_w * c_w)$$

$$V_{vt} = S_{vt} * L_{vt} / (S_w * b_w)$$

Our control surfaces were sized based on percentages of chord and span as given in lecture:

$$\begin{aligned} \text{Aileron chord} &= 25\% * c_w, \text{ Aileron span} = 35\% * b_w \\ \text{Elevator chord} &= 32.5\% * c_{Ht}, \text{ Elevator span} = 92.5\% * b_{Ht} \\ \text{Rudder chord} &= 30\% * c_{vt}, \text{ Rudder span} = 90\% * b_{vt} \end{aligned}$$

Tables AS1 and AS2 provide a broad summary of the geometric properties of our aircraft. With our geometry and weights refined to better represent our as built aircraft, we were ready to generate more aerodynamics plots and run stability tests using XFLR5. To better account for drag, we input our drag values and areas as calculated in our drag buildup. Our primary focus was to understand cruise performance, so we ran multiple fixed lift simulations to determine an ideal trim velocity.

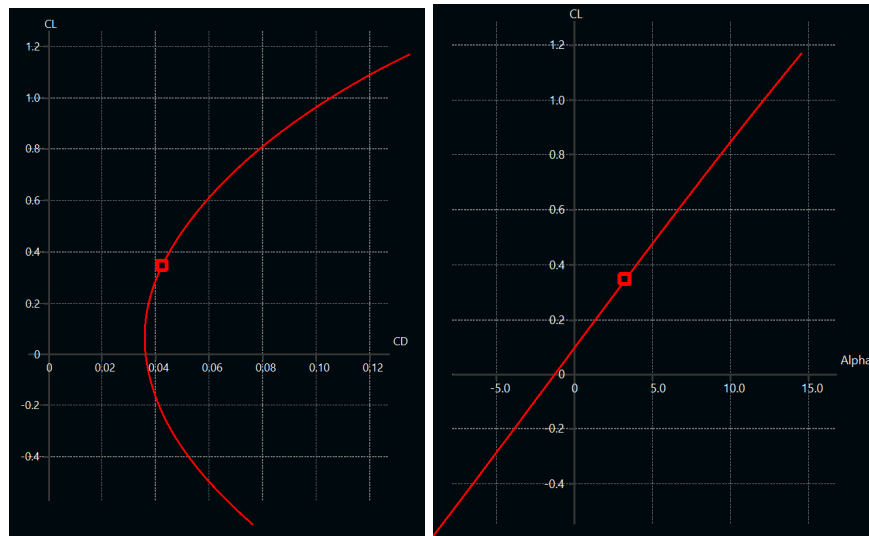


Figure 17: XFLR5 plots of Drag Polar and C_L vs. α for a 70 ft/s fixed speed simulation.

Using an XFLR5 fixed lift simulation with our aircraft weights, geometries, and extra drag surfaces included, we found our aircraft was longitudinally stable as it had a negative C_m vs alpha curve and a positive C_{mo} . We found our trim angle of attack at cruise and its associated trim velocity to be 3.25 degree and 70 ft/s respectively. The trim cruise velocity is nearly exactly what was predicted with our original value used for sizing in SRR+SDR. With our trimmed cruise speed finalized, we ran fixed speed simulations to obtain the figures shown directly above and below. All analyses were run using the Ring Vortex method in XFLR5 (vortex latus method 2).

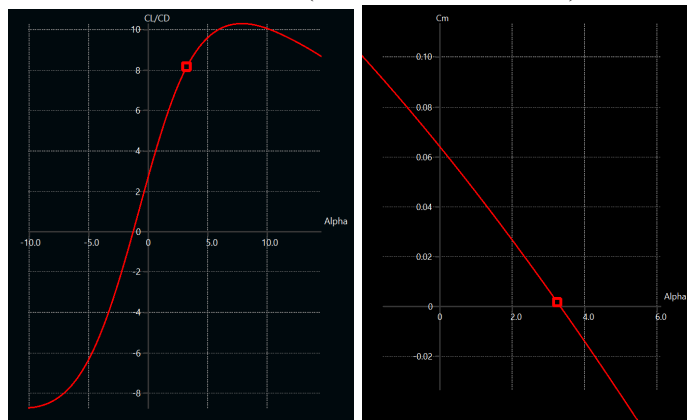


Figure 18: Modified XFLR5 Plots of L/D and C_m vs. AoA, for a 70 ft/s fixed speed simulation.

With our new configuration and our new center of gravity known, we were able to determine our static margin. Using a neutral point value of 0.503 ft aft of the leading edge obtained using XFLR5:

$$SM = (x_{NP} - x_{CG}) / c = 19.3\%$$

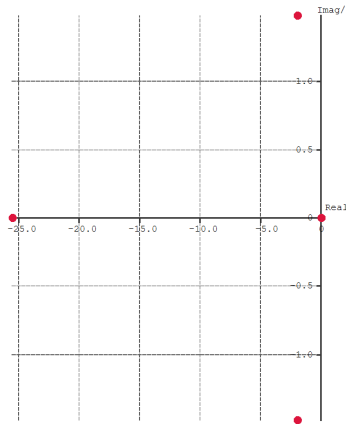


Figure 19: Root Locus for stability analysis on aircraft.

Our root locus from XFLR5 shows that all our eigenvalues have negative real components, further proving the stability of our aircraft. Below are our final design stability derivatives with associated state matrices (longitudinal and lateral):

Longitudinal derivatives		State matrices	
XU=	-0.20432	Cxu=	-0.031613
Xw=	0.89311	Cxa=	0.13819
ZU=	-4.3601	Czu=	0.013205
Zw=	-28.157	CLA=	4.3566
Zq=	-8.1637	CLq=	7.8043
Mu=	-0.010415	Cmu=	-0.0049782
Mw=	-2.4572	Cma=	-1.1745
Mq=	-3.9893	Cmq=	-11.545
Neutral Point position=	0.16522 m		
Lateral derivatives		Longitudinal state matrix	
Yv=	-2.0155	CYb=	-0.31184
Yp=	0.093091	CYp=	0.018902
Yr=	1.9194	CYr=	0.38974
Lv=	-0.22129	CLb=	-0.022467
Lp=	-3.032	CLp=	-0.40397
Lr=	0.86696	CLr=	0.11551
Nv=	1.8198	Cnb=	0.18476
Np=	-0.46913	Cnp=	-0.061305
Nr=	-1.7225	Cnr=	-0.22949
		Lateral state matrix	
		-0.413429	0.0190955
		-1.49887	-22.3749
		3.00448	-0.983195
		0	1

Figure 20: Longitudinal and Lateral stability derivatives and state matrices.

Dynamics and Control

Servo Sizing

The servos are sized such that a 30 degree deflection in the angle on the servo arm will translate to a 25 degree deflection of the control surface it is attached to, allowing for ± 25 degree deflection on the ailerons, rudder, and elevator. We intend to use one HS-311 servo to control the elevator and 3 EMAX ES08MA II servos to control each aileron and the rudder. Initially these servos were to be bought directly from the manufacturer, but it was cheaper to buy from amazon to save on shipping.

Servo	Count	Stall Torque (oz-in)	Weight (oz)	Max Current (mA)	Voltage (V)	Cost per Servo (\$)
HS-311	1	42-49	1.51	800	4.8 - 6	16.50
EMAX ES08MA II	3	21-28	0.42	500	4.8 - 6	8.99

Table 8: Servo Specifications

Additional Control Components

We also had to purchase control horns, linkages, servo extenders, and hinges as part of the control system. Hinges will be used to attach the ailerons to the wings and rudder and elevator to tail. The control horns and linkages will connect the control surfaces and servos. Finally the extenders are used to connect the servos to the receiver. Our extenders will be 3 feet long, long enough to connect the servos to the receiver under the wing connection with a margin of safety in case we decide to move the receiver's internal position.

Control Authority

To analyze control authority, we used XFLR5 to analyze performance under cruise conditions with deflected control surfaces. Even though we plan to have elevator deflection of ± 25 degrees, we had trouble getting convergence past -15 degrees, so the following plots show -15, 0, and 25 degree elevator deflection in red, green, and blue respectively.

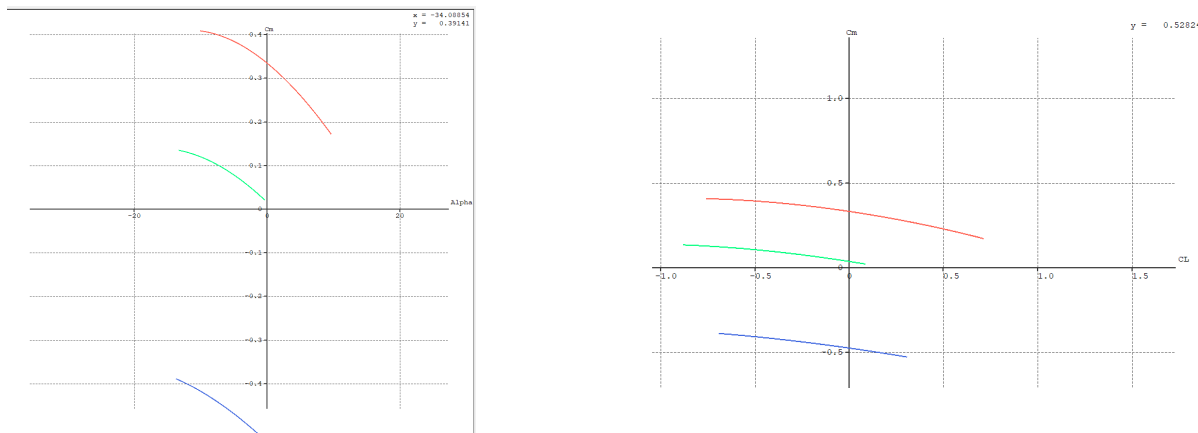


Figure 21: Moment Coefficient vs Angle of Attack(Left) Moment Coefficient vs Coefficient of Lift(Right)

These plots are not complete because of convergence issues, however we believe if we could get a full line placed for the elevator in the -25 degree position, that it would show a lift coefficient greater than 1.2 when the moment coefficient is equal to 0. This would mean that we could reach our max lift coefficient and stall the aircraft. Our lift coefficient at cruise is 0.2, and it looks like if our elevator has a slight negative deflection then CL would equal 0.2 at $C_m = 0$. These conditions fulfill control authority.

Flight Performance

With our new aircraft configuration, we would have to recalculate many of our performance quantities that were found at the time of CDR; changing our aircraft weight noticeably impacted our longitudinal stability by increasing our stall speed and thus increasing the cruise velocity we were actually able to achieve in flight tests (our first test carrying 14 payload cubes had a time of 91 seconds, whereas our second flight test carrying 29 cubes had a time of 70 seconds).

Takeoff

As was done during CDR, we were able to use our ODE45 script to determine our takeoff performance. We again estimate that one of our team members can lightly jog at 10 ft/s and throw an object vertically upward at 2 ft/s from an initial height of 6 feet (roughly head height). With these initial conditions in mind and our aircraft's aerodynamic data known from XFLR5, we were able to run a dynamic simulation using ODE45 to determine the trajectory of our aircraft at takeoff. Figure P1 in the appendix shows these results.

We used a rough estimate of the equations of motion for an aircraft at takeoff, as well as our takeoff thrust provided by eCalc to complete this simulation.

$$F_x = \text{Thrust} * \cos(\alpha) - \text{Lift} * \sin(\alpha) - \text{Drag} * \cos(\alpha)$$

$$F_y = \text{Thrust} * \sin(\alpha) + \text{Lift} * \cos(\alpha) - \text{Drag} * \sin(\alpha)$$

$$V = \sqrt{V_x^2 + V_y^2} \quad \text{and} \quad \alpha = \tan^{-1}(V_y / V_x)$$

An important caveat for these results is that the coefficients of lift and drag were constants and not functions of the changing angle of attack. This simulation was run until the Y component of velocity was no longer negative. This occurred after 0.76 seconds of flight, at which point for the sake of our flight test we will consider the takeoff segment of the mission to be completed and the climb segment to be started. Using XFLR5, we ran a fixed speed simulation at the final takeoff velocity (35.1 ft/s) to determine parameters of interest at the end of our takeoff segment. This simulation was run with elevator deflection set to 25 degrees down and aileron deflection at 20 degrees down. This configuration gives us a coefficient of lift of 1.4 at an AoA 14 degrees, which is the initial angle we will be targeting to throw our aircraft. Table P2 in the Appendix shows our adjusted flight performance values at the time of flight.

We can tabulate our aircraft's dimensionalized lift, drag, and thrust available at takeoff using the following equations:

$$\begin{aligned} \text{Lift} &= C_L q_{inf} S_{ref} \\ \text{Drag} &= C_D q_{inf} S_{ref} \\ q_{inf} &= \frac{1}{2} * V^2 * \rho \\ \text{Thrust Available} &= \text{Maximum Thrust} - \text{Drag} \end{aligned}$$

Plugging in our known values gives the dimensionalized aerodynamic forces and thrust, which can be seen in Table P3 in the appendix.

At takeoff, we will be relying on our oversized propulsion system, in other words we know that we will not be able to reach our stall speed before crashing into the ground (as can be seen from our dimensionalized lift value above being less than our aircraft's weight). We will seek to maintain an angle of attack close to that of our climb AoA so that our high thrust can be utilized to create upwards acceleration. That being said, the thrust available value above of 8.34 lb_f is misleading with the newfound context of our mission; we will be using our maximum thrust at takeoff and thus will have no extra "available" thrust during our takeoff mission segment.

From table P3 it can be noted that our stall speed decreased by nearly 10 ft/s due to the increase in payload weight. This is theoretically expected and explains our nearly 20 second decrease in mission time when increasing our payload from 14 cubes to 29 cubes. Our aircraft's max lift configuration lift curve slope can be seen in figure P4 in the Appendix.

Climb

We struggled with non-converging simulations above 15 degrees using our completed aircraft configuration in XFLR5, therefore we have decided to change our climb angle to 15 degrees rather than the 20 degrees previously discussed in our SRR+SDR report. We decided that a 25 degree aileron and elevator control surface deflection was adequate for climb. Running an XFLR5 simulation with these conditions at a fixed speed of 55 ft/s gave the performance parameters shown in table P5 of the Appendix.

With these parameters now known, we were able to determine our dimensionalized Lift and Drag values during climb (using the same equations as takeoff), the results of which are shown in Table P6 of the Appendix.

The last performance metric we wanted to find for the climb duration of our mission was our rate of climb. We felt that the easiest way to solve for this value was to use trigonometry. A right triangle can be created from our takeoff trajectory; the hypotenuse is our climb velocity (estimated to be 55 ft/s), and the angle between the horizontal and hypotenuse is our flight path angle AoA (15 degrees). Using this method, we estimate our rate of climb to be 14.24 ft/s. Assuming we climb to an altitude of 200 ft, this means our climb duration will be 14.05 seconds. Our group has concerns with determination of altitude during flight tests, and thus we will not seek to optimize flight performance as a function of altitude. That being said, our climb will stop at an altitude 200 ft at which point we will consider our aircraft to be at a cruising altitude.

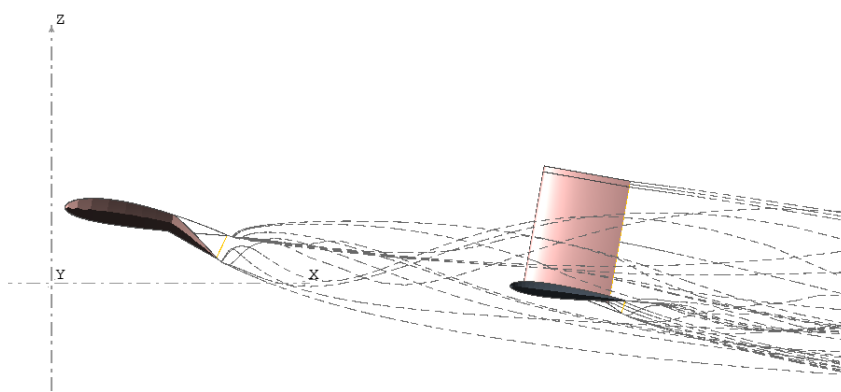


Figure 22: Streamlines in Climbing flight.

Cruise

Our finalized aircraft cruise velocity was determined in the aerodynamic section of this report to be 70.591 ft/s. Running a fixed speed simulation in XFLR5 gave the performance outputs shown in table P7. As done previously, we can find our dimensionalized lift, drag, and our thrust available at cruise, the results of which are listed in table P8 of the Appendix.

Turning

Turns for this mission had a radius of 100 ft as specified by the RFP. To start our analysis of our turning flight, we decided to deflect our ailerons by 15 degrees in opposite directions on either wing along with a 15 degree deflection of our rudder to initialize a right turn (positive yaw with z axis pointing down). What followed was an iterative process to select a sideslip angle for our turns. We ran multiple fixed lift simulations until we found a value for beta that gave us a trimmed velocity (zero moment coefficient) of 65 ft/s. We found that a sideslip of 15 degrees at an angle of attack of 2.25 degrees gave us a trimmed velocity of 65.67 ft/s. With these turning variables noted, we were able to obtain aerodynamic data for our aircraft turns, shown in Table P9 and P10 of the appendix.

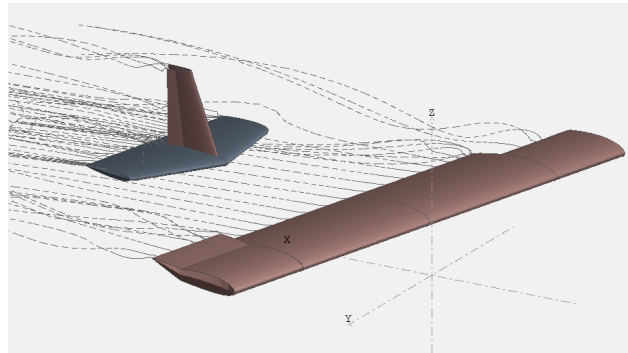


Figure 23: Original configuration turning flight control surface layout with streamlines featured.

Time of Flight:

With our mission velocities known and our flight path distance given in the RFP, we were able to breakdown the time in each mission stage:

Takeoff → 0.92 sec, Climb → 14.05 sec, Cruise → 51.51 sec, Turns → 26.93 sec.

Total TOF = 93.41 seconds. These TOF breakdowns were found using our 14 payload weight and aerodynamic parameters, and seeing as how our actual first flight test was 91 seconds, we believe these performance calculations were done correctly.

Parts Acquisition List

The parts acquisition list is listed in the figure below:

Part Name	Description
Tempest 4130-540Kv Brushless Motor	Motor
Cobra 60A ESC with 6A Switching BEC	ESC
Liperior 3300mAh 6S 30C 22.2V Lipo Battery	Battery
13x6.5E	Propeller
HS-311 Servo-Stock Rotation	Servo
EMAX ES08MA II	Servos
FOAMULAR NGX F-250 2 in. x 4 ft. x 8 ft. SSE R-10 XPS Rigid Foam Board Insulation	Foam
National Balsa	Balsa Wood
Large Size Nylon Pinned Hinges	Hinges
36" Servo Extenders	Servo Wires
Velcro Alfalock	Velcro
HobbyPark 20pcs Nylon Control Horns	Control Horns and Linkages
Nose Cone	3D-Printed Nose Cone
SPAX® #6 x 1-3/4" Combo Drive Zinc Flat Head Wood Screw - 25 Count	Screw
Hillman #6 x 32 Zinc-plated Steel Hex Nut (24-Count)	Nut
8 oz. Wood Glue/Epoxy	Glue
Monocoat	Monocoat
Rubberbands	Rubber bands
Velcro Alfalock	Velcro payload
Wood Dowel (1/8"x12 in)	Stabilizer Support
Wood Dowel (1/4"x48 in)	Stabilizer Inserts
Self-Locking 8-in Zip Tie	Zip Tie
Aluminum Foil Tape - Roll	Tape
1/4" Sanded Pine Plywood	Plywood
Painters Tape	Tape

Figure 24: Parts List(ADD new stuff from lab)

The figure shows all of the materials and items we will need to acquire for the complete construction of our aircraft. This includes components of the propulsion and control system, along with structural components including foam and woods, and items used to keep the plane together such as glue and velcro. The links to these suppliers are listed in the appendix below and they have been updated since the parts were ordered as some components and suppliers were changed to decrease shipping costs.

Prototype Fabrication, Economic, and Test Plan

The project will follow a defined schedule detailing the timeline for each component's manufacture and testing. Firstly, CDR must be completed by Wednesday October 9th. Secondly, after the completion and presentation of CDR and contingent on the design's acceptance, parts ordering must be accomplished by Monday October 21st.

Following these milestones the manufacturing process will follow the gantt chart schedule shown below in Figure 25:

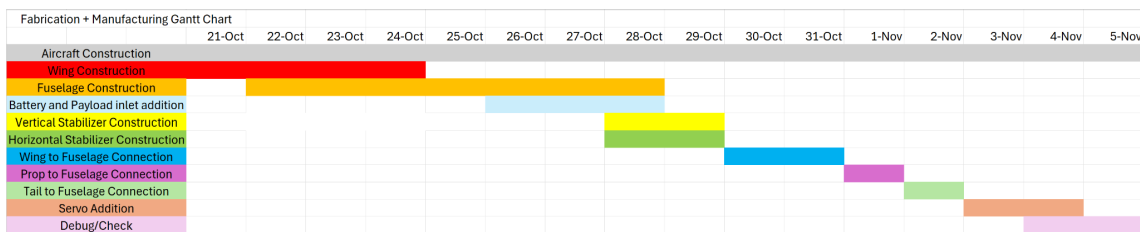


Figure 25: Manufacturing Schedule

The manufacturing process is as follows; the wings will be cut out of XPS foam using the foam cutter in the lab. We will cut not only the airfoil out of the stock but also cut the channel in which our spar will sit. The horizontal and vertical stabilizers will also utilize the foam cutter and be made of the same XPS foam. We will cut the inward facing ends of the stabilizers as required in order to secure them onto a rod connecting the two halves of the horizontal stabilizer to each other, the tail of the fuselage, and the vertical stabilizer. The fuselage will be built using laser cut

pieces of balsa and plywood which will form the ribs and horizontal structural beams. These ribs will be notched to allow them to easily fit onto the beams and glue will be used to secure their position. A layer of monocoat will be used to cover the fuselage and provide an aerodynamic skin around the ribs. A curved block will also be 3D printed which will act as the connection surface where the wing will be fastened to the fuselage via velcro. Another 3D printed block will be used to serve as the connection housing for the stabilizers. Additionally the control surfaces will be made of the same material as their main component. The control surfaces will be hand cut from their main component and be trimmed such that hinges can be attached to guide rotation. The servos will be housed within the foam airfoils by carving out the needed space and gluing them in place. Additional channels will be cut where necessary to allow the wiring to traverse.

The order of assembly will be to first assemble the fuselage. This involves gluing the ribs to the horizontal beams and applying the monocoate skin to the exterior. Then the curved block will be glued to the interior ribs and extrude through a hole in the monocoat. The motor will then be attached to the fuselage via four bolts with a nut and washer on the interior of the fuselage. Additionally zip tie the ESC to the top of the fuselage and poke a hole for the required wiring in the monocoat.

The next step is to attach the cut vertical stabilizer onto the fuselage by joining the cut slits of the vertical stabilizer with the male end of the 3D printed tail connector piece. Additionally, glue will be added to the seams as necessary. The cut horizontal stabilizer is then added in the same manner to the vertical stabilizer. Next attach the battery, receiver, and payload to the interior of the fuselage via velcro squares and wire as needed.

The next step is to attach velcro to the 3D printed curved portion of the fuselage and the opposing surface of the wing which contacts that surface. After the adhesive settles the two sections can be connected and rubber bands can be stretched across the top surface of the wing in an “X” shape and be hooked onto the extruding pins from the fuselage. The cost breakdown is shown below in Figure 27. The cost is broken down by individual components and location ordered from.

Part Name	Description	Total Cost (\$)	Supplier
Tempest 4130-540Kv Brushless Motor	Motor	76.49	Cobra
Cobra 60A ESC with 6A Switching BEC	ESC	37.49	Amazon
Liperior 3300mAh 6S 30C 22.2V Lipo Battery	Battery	51	RC Battery
13x6.5E	Propeller	5.73	APC Propellers
HS-311 Servo-Stock Rotation	Servo	16.5	Amazon
EMAX ES08MA II	Servos	26.97	Amazon
FOAMULAR NGX F-250 2 in. x 4 ft. x 8 ft. SSE R-10 XPS Rigid Foam Board Insulation	Foam	46.48	Home Depot
National Balsa	Balsa Wood	31.44	Balsa Wood
Large Size Nylon Pinned Hinges	Hinges	8.99	Amazon
36" Servo Extenders	Servo Wires	17.99	Amazon
Velcro Alfatlock	Velcro	6.68	Amazon
HobbyPark 20pcs Nylon Control Horns	Control Horns and Linkages	8.97	Amazon
Nose Cone	3D-Printed Nose Cone	15.00	3D Print
SPAX® #6 x 1-3/4" Combo Drive Zinc Flat Head Wood Screw - 25 Count	Screw	3.1	Lab
Hillman #6 x 32 Zinc-plated Steel Hex Nut (24-Count)	Nut	1.48	Lab
8 oz. Wood Glue/Epoxy	Glue	4.97	Home Depot
Monocoat	Monocoat	16.99	Amazon
Rubberbands	Rubber bands	1	Lab
Velcro Alfatlock	Velcro payload	3.5	Amazon
Wood Dowel (1/8"x12 in)	Stabilizer Support	0.24	Lab
Wood Dowel (1/4"x48 in)	Stabilizer Inserts	0.94	Lab
Self-Locking 8-in Zip Tie	Zip Tie	0.06	Lab
Aluminum Foil Tape - Roll	Tape	1.24	Lab
1/4" Sanded Pine Plywood	Plywood	1.17	Lab
Painters Tape	Tape	1	Lab
Total		385.42	

Figure 26: Cost Breakdown by Component

Following the manufacturing process we plan to conduct a static test of our propulsion and control surfaces. We will statically hold the aircraft and test the propulsion at the different levels of thrust that the craft will face in flight. We will also actuate the control surfaces to verify that they are both responsive and actuate to the degree required.

As-Built Aircraft Description



Figure 27: Fully Assembled Plane Flight Ready

The above image shows the fully assembled plane in its final configuration. There is a rectangular foam wing connected to the fuselage on top of the white 3-D printed piece using rubber bands and velcro as seen in the image. The fuselage is made out of balsa and plywood and is covered with a blue Monokote wrap. The battery is attached just behind the motor using the hatch on the side of the fuselage for access. The motor is connected to the ESC which is resting on top of the nose part of the fuselage with the wiring zip tied to the fuselage to secure them. Right below the ESC is our payload storage which stored 14 payloads for the first flight. The payloads are secured using blue tape seen under the ESC. All of the airfoils are taped at the trailing edge to prevent any tearing of the foam at the edge as the trailing edges are very thin. The servos for the wing are underneath the wing, for the horizontal stabilizer the servo is on top and the vertical stabilizer servo is on the side. These servos are connected to the foam using hot glue and tape. All the wiring for the servos to the receiver are below the wing or through the tail fuselage and are taped to surfaces to make sure they are secure. The receiver sits right under the plane and can also be accessed using the hatch. Further description of the assembly of the plane and its manufacturing is described below.

Flight Test Data Tables

While many important geometric, mass, and structural values remained the same during our transition from CDR to manufacturing, there were some small changes that our group chose to make to ease manufacturing difficulties and to attempt to maximize our overall flight test score. A comprehensive set of tables are available in the Appendix labeled AB (as built), and give detailed quantitative values of all important characteristics of our as-built aircraft.

Vehicle Manufacturing

The first step in the manufacturing process was to build and assemble the fuselage. The process began with laser cutting the required number of ribs and stringers at Bechtel Innovation and Design Center. The majority of the ribs and spars were made of balsa wood, and the nose section was made of plywood. These laser cut pieces were then meticulously assembled and glued at each joint. This was done in three sections; a tail section which corresponded to one half of the spar, a payload section to be attached under the 3D printed wing support at a later time, and finally the plywood nose section which corresponded to the other half of the spar. Next the two spar pieces were precisely cut and sanded as needed to fit within the three 3D printed pieces. It was then glued through the middle of the assembled ribs for its corresponding section as the main support stringers. Balsa sheets were then cut to match the taper of the tail and glued to each side of the tail spar as added support. Finally, a payload door was made, it was cut from plywood by hand and velcroed to the side of the payload section of the fuselage.



Figure 28: Fuselage Sections

While this painstaking process was taking place the main wing was also in the manufacturing stage. The main wing was cut using the foam cutter and consisted of two halves. The foam cutter was programmed to cut the airfoil designated in CDR as well as a rectangular cut out at quarter chord along the bottom large enough to house our spar. After the wing sections were cut they were glued together to form a wing that was the desired span. Next a spar was cut from the purchased stock. Due to the size of the purchased stock the spar had to be made in three pieces. Each piece was notched such that it could be fastened to the others forming one spar that matches the required span. The spar was then adhered to the main wing using the rectangular cut channel. Finally a layer of tape was secured to the trailing edge of the wing in an effort to protect it as it was noticeably fragile.



Figure 29: Main Wing

The motor was fastened to the front plate of the fuselage and fastened into place. The propeller was added to the front of the motor and removed as needed for assembly of other components.



Figure 30: Motor Assembly

Next, the wing connection piece was manufactured. This piece was 3D printed and its purpose was to serve as the connection point between the fuselage and wing. It also provided additional support to the entirety of the aircraft and helped secure the three fuselage pieces together. The body was too large to print in a single print so it was printed in halves with one end having a male component and the other having a female component. After printing, glue was added to the joint and the two halves were fastened together. Then the payload section of the fuselage is glued to the underside of the printed component. Next the pins were glued through the fuselage and to the underside of the pointed part. The nose and tail were then secured to the print by inserting the spar through the printed channel and gluing along any interface. Additionally, all wood connections between fuselage sections were glued together. Finally, velcro was glued to the top surface of the printed component and to the underside of the main wing.

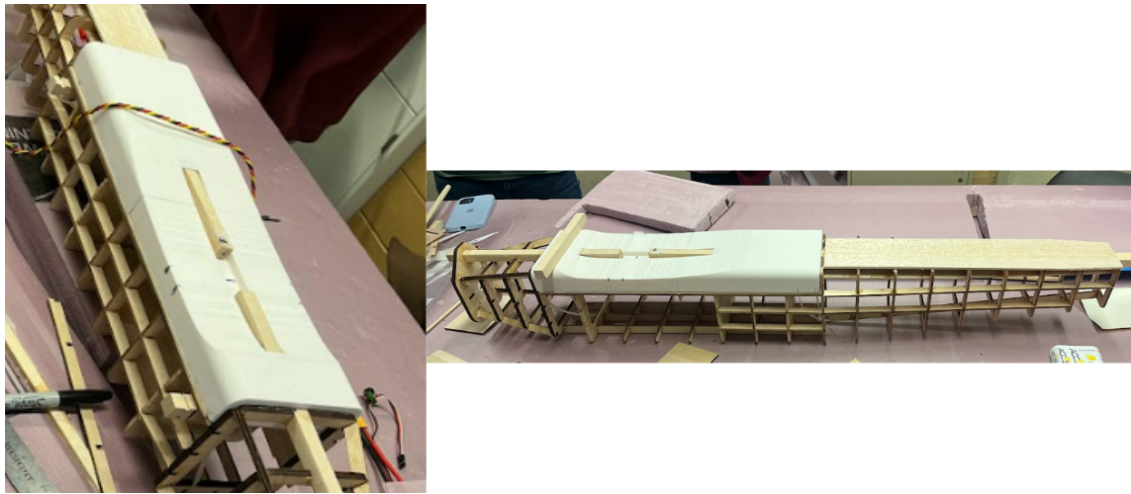


Figure 31: Wing Connector Component

Additionally, a tail connection piece was 3D printed. The piece served as the connection point between the tail spar, the vertical stabilizer, and the horizontal stabilizer. The tail connection piece was printed in two halves such that it can be assembled around the tail spar. It was fastened to the tail spar with two bolts along with the equal number of washers and nuts, glue was added as an additional layer of adhesive. A wooden dowel was cut into six pieces to be used to secure the stabilizers in place. These dowel pieces were glued into their matching holes on the printed part.

The horizontal and vertical stabilizers were next manufactured utilizing the foam cutter. Due to the foam cutter no longer being able to be programmed to cut, a stencil was made using leftover material. Each stabilizer had a stencil glued on either side of a stock block of foam and these were used to guide the manual cutting of the stabilizer with the hot wire. The stencil also included a cut which hollowed out a section of the foam in which the wood dowels of the connection piece will fit. They were then glued in place onto those dowels. Additionally, small wood dowels were

glued to the ends of the horizontal stabilizer and to the tail of the fuselage. The purpose of this was to help the stability of the tail and to hold the horizontal stabilizer level to the fuselage.



Figure 32: Aircraft Tail Assembly

To make the control surfaces, we would first measure out and mark an area of the wing or stabilizer to be cut out. The sizes and positions of these surfaces were outlined in the CDR. The sections were then cut with an exacto knife or box cutter. To allow for full 25 degree deflection in either direction, we then shaved off a portion of the control surface near the hinge point. The surfaces were then attached to the wing or stabilizer with glued and taped hinges.



Figure 33: Control Surfaces

Monocoat was then added to the surface of the fuselage. This process was slowly done using small sections of monocoat at a time and slowly heating and stretching the monocoat to fully wrap the fuselage.



Figure 34: Monocoat application on fuselage.

The servos were first connected to the push rods and control horns. One horn was to be connected to the control surface and the other would be connected to the servo and screwed in. The servo horns also needed connector linkages to the push rods. Initially, these linkages were too big to fit in the servo horns, so the control horn holes were widened with a 3/32 drill bit. The linkages were then attached with two washers and a nut each. Later, these were sealed with Loctite. Once everything was assembled we positioned the servos and horns and performed a controls test to confirm we had the right orientation. We first attached the control horns to the control surfaces by poking them into the foam and using glue and tape. Then we outlined our servo position and made a hole for the servo to fit before glueing in the servo. We used hot glue for this as it held up nicely in the foam.

The wiring for the rudder and elevator servos were fed through the fuselage before monocoating and were later attached to the receiver and servos. The aileron servos had their wires attached to the wing with tape. When the wing was separated from the fuselage these wires would remain attached to the wing and be disconnected from the receiver.



Figure 35: Servo and Wiring Example

The ESC was added to the top of the spar at the nose via zip tie. The receiver and battery were secured within the fuselage by velcro such that they were secure in place during flight but easily removable as needed. Payload could be added in two places. Firstly in the compartment in the nose which 14 payload cubes could be stacked and a layer of tape was added over the compartment to secure them. Secondly, a small balsa box was glued together and then glued into the inside of the fuselage under the wing where 18 additional payload cubes could be added via the payload access door.



Figure 36: ESC Location

When we had to fly, the wing would first be attached, and wires connected. Then we would add and secure our battery and payload in under five minutes. We used tape to secure the payload in the nose of the aircraft and velcro to secure things in the fuselage.

Design Modifications Post CDR

During the manufacturing process several small changes were made from the initial design outlined in CDR. Firstly, the push rods and control horns were originally to be bought from amazon, but they were out of stock by the time purchasing tried to order them, so instead we had permission to use push rods, horns, and linkages from the lab.

When first constructing our fuselage we observed how brittle and malleable the balsa wood stringers and ribs were. We decided in order to further strengthen our aircraft and ensure it could survive both flight conditions and a belly landing the team decided to change a couple things. Firstly, a wooden spar made from the spare material for the wing spar was added in place of the top stringers. Secondly, we decided that with the weight of the motor and payload being primarily located at the nose of the aircraft we should spend the money to make this section stronger and use plywood instead of balsa. Third, the team glued balsa sheets around the spar in the tail in an effort to further strengthen the weaker tail section of the aircraft.

Another aspect that was changed due to concerns of structural integrity was the tail connection. Initially it was planned that the vertical and horizontal stabilizers would meet and be fastened to the balsa tail section of the fuselage. However, with the concerns regarding the strength of such small balsa pieces another solution was needed. With the addition of the wooden spar a 3D printed part was designed and manufactured. This part was printed on two pieces and fastened around the tail spar and allowed for wooden dowels to be glued in place which the stabilizers were able to attach too.

Another important change we had to make was to un-taper our horizontal and vertical tail. This change was made due to the hot wire foam cutter being taken out of commission due to internal sabotage. We knew that a tapered tail would be incredibly difficult to hand cut, so we decided to use the mean chord for both the horizontal and vertical tail and simply make rectangular tails.

After completion of the horizontal stabilizer it was discovered that the horizontal stabilizer was at a slight angle due to the warping of the wooden spar. Two small wooden dowels were glued to each end of the horizontal stabilizer (top and bottom) and attached to the end of the balsa rib fuselage. They were glued in such a way to realign the stabilizer and correct the warping.

Due to concerns around our center of gravity location, we were forced to make last minute design changes to our payload storage method and location. Originally, we were going to place a foam box with 4 payload units under the leading edge of our wing, but changes to our tail caused our aircraft to be far too tail heavy. To combat this fatal flaw, we moved our payload storage to our plywood nose. Not only did this change allow us to add more payload units to our

aircraft, but it increased our stall speed which in turn increased our cruise speed, allowing us to achieve a far higher score than we ever would have been able to with our original design.

Description of Flight Test

The flight test was a very successful and positive experience for the team. Prior to the flight, the team had to pass the Flight Readiness Review (FRR), which included critical tests such as the wing tip test, shake test, and several other essential checks to ensure the aircraft was ready for flight. Once the aircraft passed these tests, additional pre-flight preparations were conducted at the airfield, including quick payload and battery loading (under 5 minutes) and a controller check to verify that the motor and servos were functioning correctly. With these steps completed, the team received the green light to proceed with the flight.

The aircraft was piloted by the lab instructor and followed the sequence outlined in our CONOPS. After the plane was launched, it immediately climbed to a stable altitude and successfully performed the required turns during the mission. The lab instructor was also able to execute the landing well, which allowed our plane to belly land and survive in one piece. The flight was extremely stable, even through strong natural winds affecting our aircraft. During the flight, the plane carried a total of 14 payload cubes for a total payload weight of approximately 30.5 ounces (1.91 lbs). The aircraft completed three laps, with the entire flight lasting 90 seconds.

The results of the flight test were promising. The score came out to approximately 0.339, a strong showing for the team. This indicates that the aircraft was able to carry a substantial payload, while also performing at a relatively efficient rate. The success of this test demonstrates the effectiveness of our design in terms of both payload capacity and flight time.

After the original flight test, teams were given the opportunity to fly again with more payload. Following this news, the team made some calculations and ran numbers regarding the weight of the plane, the aerodynamic stability using XFLR, propulsion, and structural integrity of the plane to figure out what payload we could use. We realized after this process that we could theoretically increase the number of payload cubes to the max (29 cubes) for a total payload weight of 63.2 ounces, which is a little less than 4 lbs. The plane passed the airfield checks, and was also able to successfully complete the mission of 3 laps around the airfield, this time in 70 seconds, giving us a score of 0.903. Given that this flight test was a more risky approach to the mission rather than the calculated one the team had prepared for, and considering that the reasons behind the more complex configuration choices were much harder to justify, we decided not to highlight this second flight test throughout our report.

Key Lessons Learned

The process of designing, building, and flight-testing our aircraft provided our team with valuable lessons in engineering, teamwork, and problem-solving. One of the most significant lessons learned was the importance of adaptability in the design process. After our CDR, we encountered several structural and aerodynamic challenges that necessitated modifications, such as the inclusion of a 3D-printed tail connector piece and balsa sheets for added support in the fuselage. These changes improved the structural integrity of the aircraft and reinforced the need for flexibility when unforeseen issues arise.

Another key takeaway was the critical role of manufacturability and precision in design execution. Our original design for a tapered tail had to be simplified to a rectangular structure due to limitations in available tools, emphasizing the importance of considering manufacturing constraints during the design phase. Similarly, the addition of support dowels for the horizontal stabilizer highlighted the need for practical, simple solutions to address stability challenges.

We also learned the importance of pre-flight readiness and iterative testing. The payload location and method were modified post-CDR after center-of-gravity testing revealed imbalances. This demonstrated the value of early testing to identify potential design weaknesses before final assembly.

Lastly, the ability to adapt to material availability was crucial. For instance, the shift from purchased control horns to lab-supplied alternatives due to stock issues underscored the need for contingency planning. Overall, this project reinforced the need for iterative design, effective communication, and the ability to innovate within constraints.

Appendix

Code:

[AAE451_SeniorDesign](#)

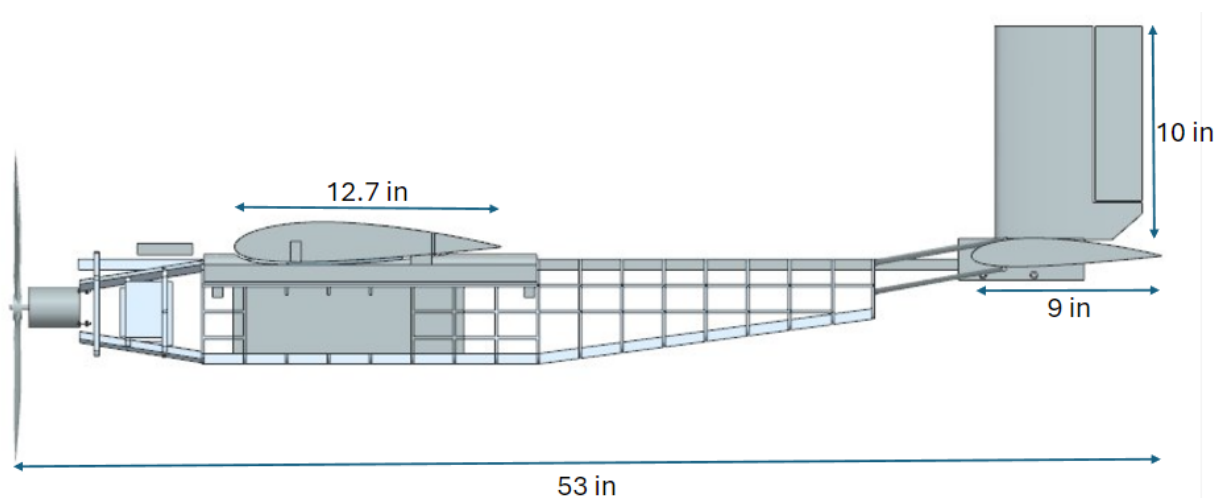
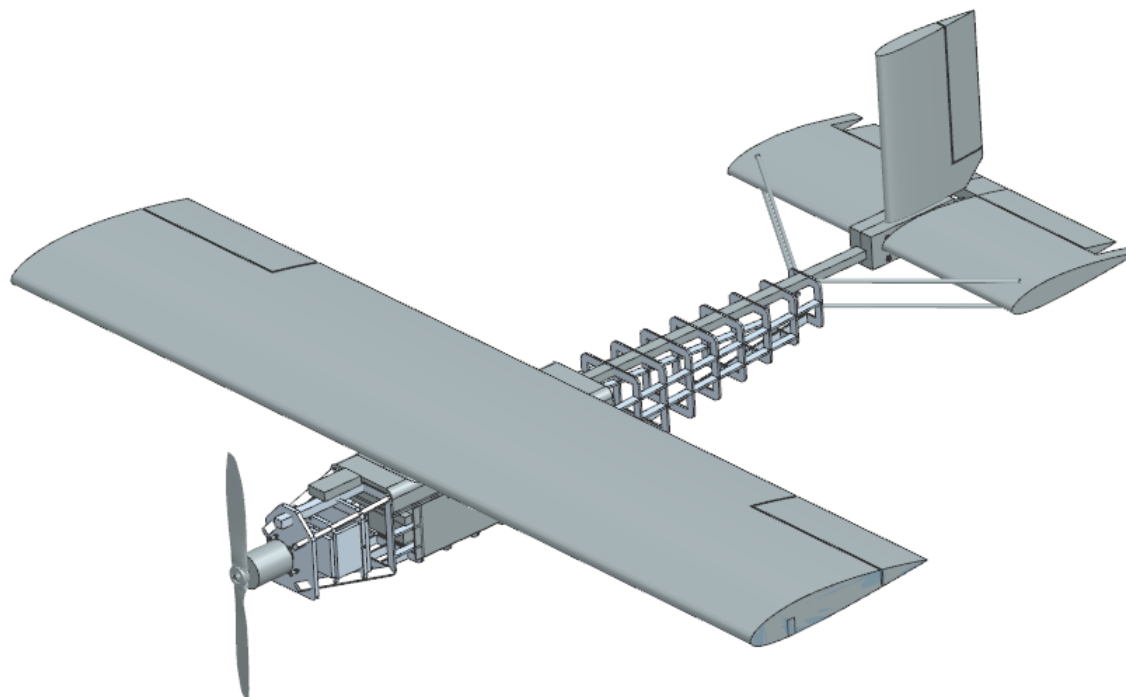
XFLR5:

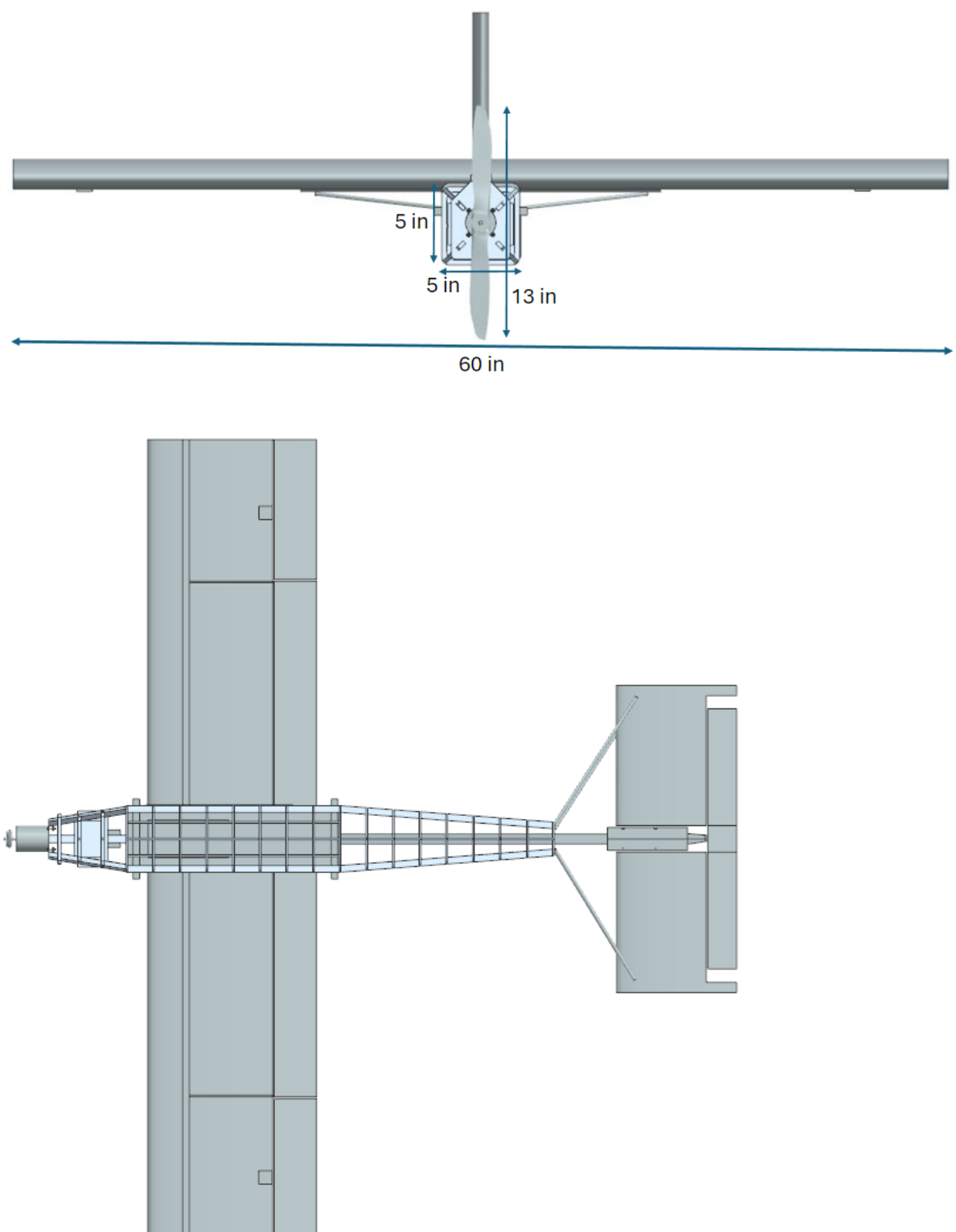
[HighWing.xfl](#)

Part Acquisition List (with links):

Part Name	Description	Total Cost (\$)	Supplier
Tempest 4130-540Kv Brushless Motor	Motor	76.49	Cobra
Cobra 60A ESC with 6A Switching BEC	ESC	37.49	Amazon
Liperior 3300mAh 6S 30C 22.2V Lipo Battery	Battery	51	RC Battery
13x6.5E	Propeller	5.73	APC Propellers
HS-311 Servo-Stock Rotation	Servo	16.5	Amazon
EMAX ES08MA II	Servos	26.97	Amazon
FOAMULAR NGX F-250 2 in. x 4 ft. x 8 ft. SSE R-10 XPS Rigid Foam Board Insulation	Foam	46.48	Home Depot
National Balsa	Balsa Wood	31.44	Balsa Wood
Large Size Nylon Pinned Hinges	Hinges	8.99	Amazon
36" Servo Extenders	Servo Wires	17.99	Amazon
Velcro Alfalock	Velcro	6.68	Amazon
HobbyPark 20pcs Nylon Control Horns	Control Horns and Linkages	8.97	Amazon
Nose Cone	3D-Printed Nose Cone	15.00	3D Print
SPAX® #6 x 1-3/4" Combo Drive Zinc Flat Head Wood Screw - 25 Count	Screw	3.1	Lab
Hillman #6 x 32 Zinc-plated Steel Hex Nut (24-Count)	Nut	1.48	Lab
8 oz. Wood Glue/Epoxy	Glue	4.97	Home Depot
Monocoat	Monocoat	16.99	Amazon
Rubberbands	Rubber bands	1	Lab
Velcro Alfalock	Velcro payload	3.5	Amazon
Wood Dowel (1/8"x12 in)	Stabilizer Support	0.24	Lab
Wood Dowel (1/4"x48 in)	Stabilizer Inserts	0.94	Lab
Self-Locking 8-in Zip Tie	Zip Tie	0.06	Lab

Aluminum Foil Tape - Roll	Tape	1.24	Lab
1/4" Sanded Pine Plywood	Plywood	1.17	Lab
Painters Tape	Tape	1	Lab
Total		385.42	





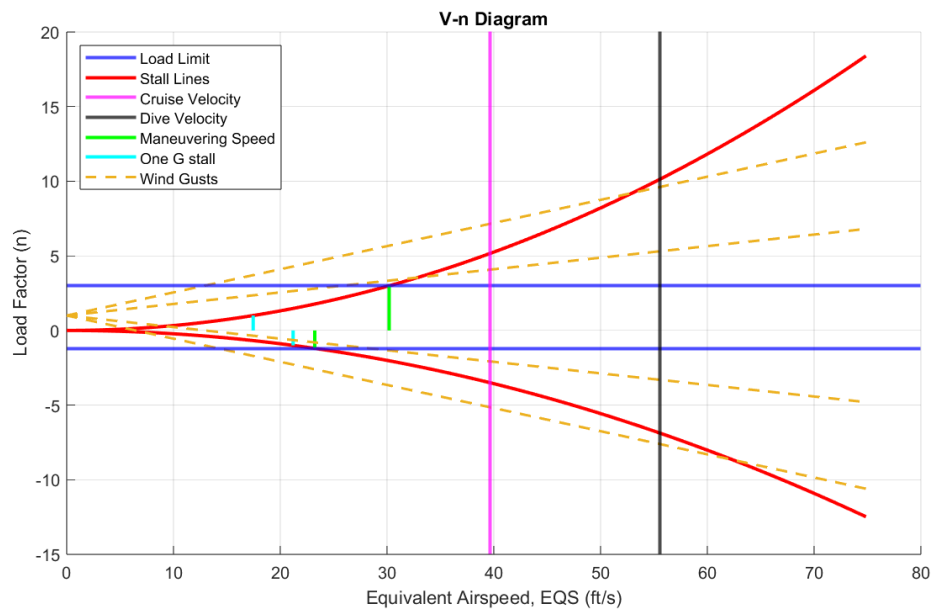
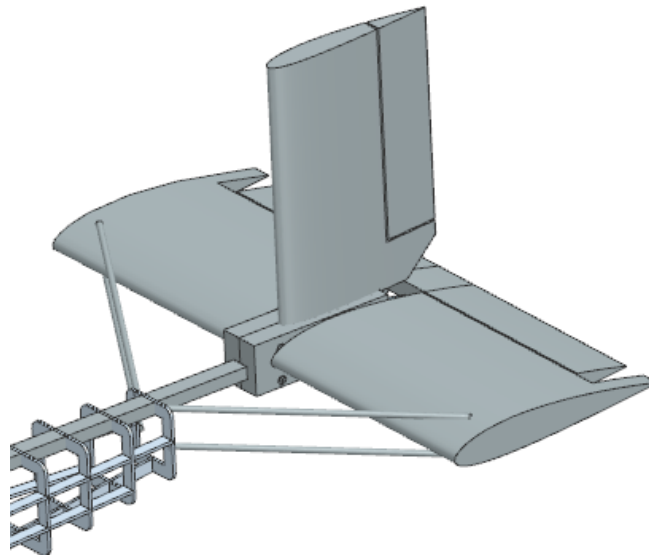
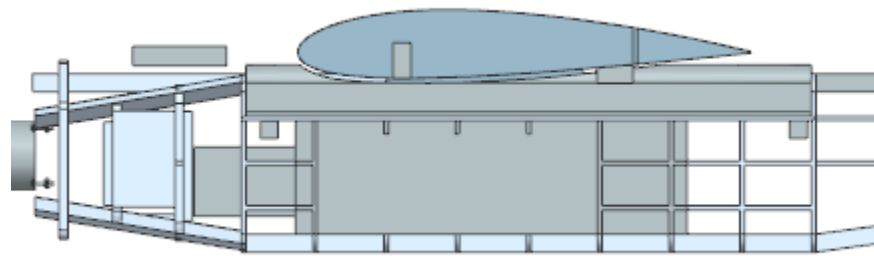


Figure V1: V-n Diagram for final design.

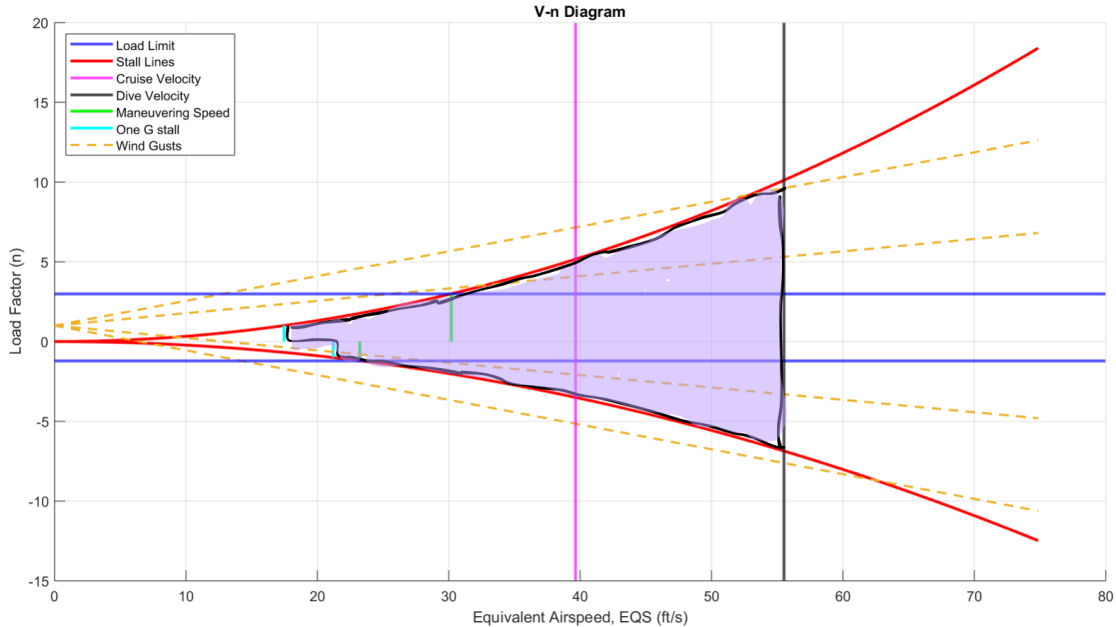


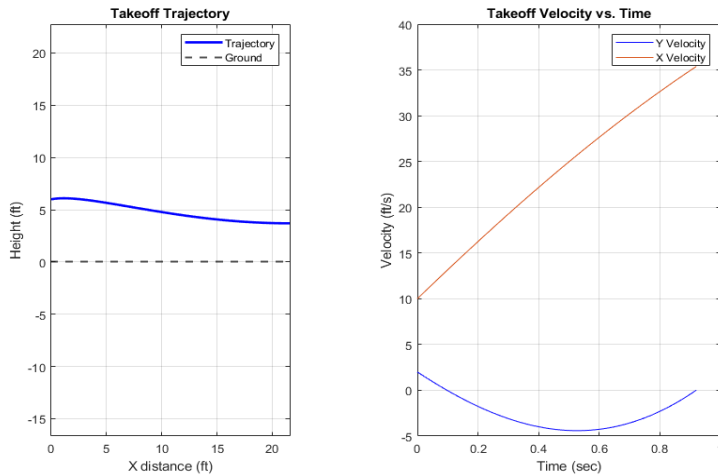
Figure V2: V-n Diagram for final design with limits.

Wing Area	5.32 ft ²	Wing Span	5 ft
Wing Chord	1.06 ft	Wing Taper	1 ($c_r = c_t$)
Horizontal Tail Mean Chord	0.76 ft	Horizontal Tail Span	1.78 ft
Horizontal Tail Area	1.35 ft ²	Horizontal Tail Aspect Ratio	2.35
Horizontal Tail Volume Coefficient	0.6	Horizontal Tail Taper Ratio (with build modifications)	1
Vertical Tail Mean Chord	0.53 ft	Vertical Tail Span	0.80 ft
Vertical Tail Area	0.42 ft ²	Vertical Tail Aspect Ratio	1.5
Vertical Tail Volume Coefficient	0.04	Vertical Tail Taper Ratio (with build modifications)	1
Fuselage Length	4.2 feet	Fuselage Diameter	10 inches

Table AS1: Geometric summary for aerodynamic surfaces.

Aileron Span	1.75 ft	Aileron Chord	0.266 ft
---------------------	---------	----------------------	----------

Elevator Span	1.65 ft	Elevator Chord	0.247 ft
Rudder Span	0.72 ft	Rudder Chord	0.159

Table AS2: Control Surface geometries.**Figure P1:** ODE45 simulation results for takeoff - adjustments made for post CDR changes.

C_L	C_D	L/D	C_m	AoA	V
0.546	0.102	5.35	-0.482	0 deg	35.1

Table P2: Adjusted performance values at the end of takeoff.

Lift	Drag	Thrust Available
8.84 lb _f	1.600 lb _f	8.34lb _f

Table P3: Adjusted dimensionalized Lift and Drag and Thrust available at takeoff.

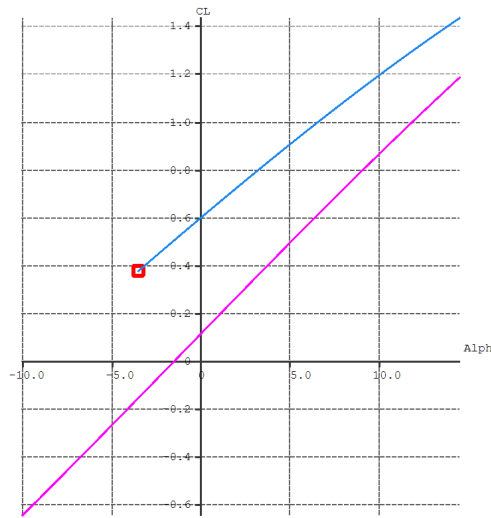


Figure P4: C_L vs. α curve for aircraft with no deflection (purple curve) and max lift deflections (blue curve)

C_L	C_D	L/D	C_m	AoA	V
1.38	0.267	5.17	-0.707	15 deg	55 ft/s

Table P5: Adjusted performance values during climb.

Lift	Drag	Thrust Available
26.43 lb _f	5.415 lb _f	4.415 lb _f

Table P6: Adjusted Dimensionalized Lift and Drag and Thrust available at climb.

C_L	C_D	L/D	C_m	AoA (trimmed)	V
0.1919	0.0362	5.38	0	1 deg	70.591 ft/s

Table P7: Performance values at cruise.

Lift	Drag	Thrust Available
7.208 lb _f	1.36 lb _f	7.99 lb _f

Table P8: Dimensionalized Lift and Drag and Thrust available at cruise.

C_L	C_D	L/D	C_m	AoA (trimmed)	V
0.2629	0.067	3.92	0	2.25 deg	65.67 ft/s

Table P9: Performance values during turns..

Lift	Drag	Thrust Available
7.208 lb _f	1.83 lb _f	7.52 lb _f

Table P10: Dimensionalized Lift and Drag and Thrust available during turns.

Wing Area	5.32 ft ²	Wing Span	5 ft
Wing Chord	1.06 ft	Wing Taper	1
Horizontal Tail Chord	0.76 ft	Horizontal Tail Span	1.78 ft
Horizontal Tail Area	1.35 ft ²	Horizontal Tail Aspect Ratio	2.35
Horizontal Tail Volume Coefficient	0.6	Horizontal Tail Taper Ratio	1
Vertical Tail Mean Chord	0.53 ft	Vertical Tail Span	0.80 ft
Vertical Tail Area	0.42 ft ²	Vertical Tail Aspect Ratio	1.5
Vertical Tail Volume Coefficient	0.04	Vertical Tail Taper Ratio (with build modifications)	1
Fuselage Length	4.33 feet	Fuselage Diameter	10 inches

Aileron Span	1.75 ft	Aileron Chord	0.266 ft
Elevator Span	1.65 ft	Elevator Chord	0.247 ft
Rudder Span	0.72 ft	Rudder Chord	0.159

Table AB1: Geometric Characteristics of built aircraft.

Structures	Weight lb _f	Propulsion	Weight lb _f
Wing	1.76	Motor	0.88
Tail	0.86	ESC	0.13
Fuselage	1.70	Propeller	0.07
Wood Glue	0.18		
Equipment	Weight	Equipment	Weight
Aileron Servos (and wiring)	0.10	Rudder Servo (and wiring)	0.05

Elevator Servo (and wiring)	0.11	Receiver	0.03
-----------------------------	------	----------	------

Total Empty Weight	5.77
--------------------	------

Useful Load	5.02
Payload	3.95
Battery	1.07

Total Gross Weight	10.89
--------------------	-------

Finalized CG was 0.5 inches aft of the leading edge → 3.68 inches aft of wing LE

Table AB2: Finalized flight test weight table.

I_{xx}	I_{yy}	I_{zz}	I_{xz}
3.27 lb _m -ft ²	12.16 lb _m -ft ²	10.95 lb _m -ft ²	14.25 lb _m -ft ²

Table AB3: Finalized flight test inertia table.

Longitudinal derivatives		Lateral derivatives	
Xu=	-0.20432	Cxu=	-0.031613
Xw=	0.89311	Cxa=	0.13819
Zu=	-4.3601	Czu=	0.013205
Zw=	-28.157	CLa=	4.3566
Zq=	-8.1637	CLq=	7.8043
Mu=	-0.010415	Cmu=	-0.0049782
Mw=	-2.4572	Cma=	-1.1745
Mq=	-3.9093	Cmq=	-11.545

Table AB4: Finalized flight test stability derivatives